

# SOLAR DESALINATION MANAGEMENT TO FULFILL GREENHOUSE WATER DEMAND USING PREDICTIVE CONTROL

Lidia Roca<sup>1</sup>

<sup>1</sup>CIEMAT - Plataforma Solar de Almería, ctra. de Senés km. 4,5 Tabernas (04200) Almería,  
lidia.roca@psa.es

Jorge A. Sánchez<sup>2</sup>, Francisco Rodríguez<sup>2</sup>, Javier Bonilla<sup>3</sup>

<sup>2</sup> Universidad de Almería, ctra. Sacramento s/n, (04120) Almería, {jorgesanchez, ffrrodrig}@ual.es

<sup>3</sup> CIEMAT - Plataforma Solar de Almería, javier.bonilla@psa.es

## Abstract

*This paper proposes a control strategy for a solar desalination plant included in a micro-grid framework. The goal of the controller is to maintain a volume of distillate despite the water demanded by a greenhouse and taking into account solar irradiance disturbances. In a top layer, the temperature setpoints are calculated to assure enough energy and reach the water requirements. NMPC is used to estimate the optimal solar field setpoints and a PI controller to choose the setpoint for the distillate unit. In a second layer, these two temperatures are controlled by the solar field pump and by a three-way regulation valve respectively. Simulation results are included to compare the proposed strategy with an open-loop operation.*

**Keywords:** NEPSAC, feedback linearization, multi-effect plant.

## 1 INTRODUCTION

Modern agricultural systems are characterized by the intensive and optimal use of land and water, turning agricultural exploitation into a semi-industrial concept. Greenhouses are systems suitable both for zones with unfavorable climatic conditions - allowing crop growth regardless of the ambient temperature, and for regions with less restrictive weather - with the aim in this case of increasing crop productivity and improving fruit quality. The greenhouse environment is ideal for farming because these variables can be manipulated to achieve optimal growth and plant development. This manipulation requires energy consumption, depending on the crop's physiological requirements and, additionally, depending on the production patterns adopted for yield quantity and timing. Crop growth is primarily determined by climatic variables of the environment and the amount of water and fertilizers applied through irrigation. Therefore, controlling these variables allows the control of the growth. The produc-

tivity optimization through efficient and adequate irrigation is a basic objective in those countries with water limitations. Furthermore, this resource limitation is made worse due to the recent rapid expansion of the surface area occupied by greenhouses in the Mediterranean Basin. Consequently, this has also led to water becoming a more important consideration in the sustainability of the greenhouse-based system in south-eastern Spain. This water deficit has been progressively depleting the aquifers in the area [19]. Eighty per cent of the irrigation water used in Almería (Spain) comes from underground sources, leading to localized overexploitation of aquifers [7]. Over the last few years, as in other arid and semi-arid areas of the world, it has been promoted the use of alternative water sources such as purified water, rain and condensed water collection as a secondary source, the reuse of drainage water, the development of new technologies related to water-use efficiency such as advanced irrigation controllers, and sea water desalination.

In this line, the idea of integrating solar desalination systems in the agricultural environment has been significantly considered with the aim of dealing with water limitations in some regions of the planet. One of the most simple and cheap techniques, the solar stills [10], can be easily combined with greenhouses [4]. This kind of distillation processes are usually located on the roof of greenhouses where a glass system is installed. Seawater is pumped to this cover where vapor is produced and raised by natural convection to the top glass where it condenses. The water falls down the roof being finally collected. As explained in [4], water produced by a solar still is not enough for growing a crop. Moreover, operational reasons, such as salt accumulation, have lead to the non real applicability of this method. A relative new concept is the use of seawater for cooling and humidification [8]. The purpose is to create adequate temperature conditions for the crops. Solar energy is used in an evaporation process to humidify water. The process is explained in [12]. The air inside the

greenhouse is cooled due to a first evaporator located at the front wall of the greenhouse. The air passes through the crops and reaches a second evaporator with hot water flowing inside it. Therefore, the air becomes hotter and more humid. This air passes finally through a condenser obtaining water from the air stream. Based on this concept, a new design has been recently proposed [27] which includes an improved solar water heater.

This paper deals with a different combination of greenhouse and solar desalination. It consists in taking advantage of the water produced in a solar multi-effect desalination, MED, plant to feed a greenhouse located in the southeast of Spain. The challenge is to properly operate the desalination plant to produce the daily water demanded by the crop.

Most of the optimization algorithms applied to desalination processes deal with the design of cogeneration plants [9, 18, 23, 26]. The objective function includes thermodynamic and environmental issues. However, few optimization problems are focused on satisfying a variable water demand. In [22], for example, a nonlinear programming, NLP, problem is defined to reduce operating costs in a reverse osmosis, RO, system. The outputs of the optimization are the number of membranes used in the operation, the feed pressure and the flow. In the present paper a Nonlinear Model Predictive Control, NMPC, is applied to find a proper temperature setpoint in a solar field coupled to a desalination process. The idea is to maintain a desired volume of distillate obtained with a MED unit despite the water consumption by irrigation in a greenhouse.

## 2 CASE STUDY

The case study explored in this paper is a micro-grid framework in which two interconnected plants must be managed; a greenhouse and a solar desalination plant (see Fig.1). On one hand, the greenhouse daily demands fresh water for irrigation purposes and, on the other hand, a solar desalination plant produces distillate water in a multi-effect distillate unit. An intermediate storage tank is assumed to be located between the production process and the consumer system.

### 2.1 SOLAR DESALINATION FACILITY

The desalination plant used in this study is the AQUASOL system sited at Plataforma Solar de Almería in the southern of Spain. This pilot plant includes a MED unit coupled with a solar collector

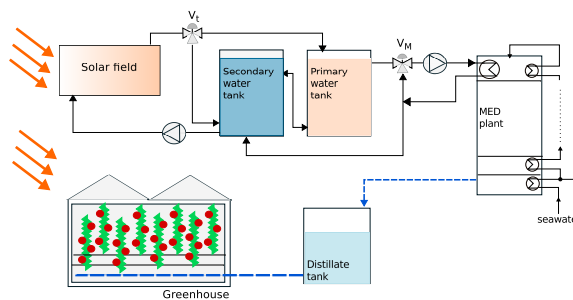


Figure 1: Solar desalination plant coupled with a greenhouse.

field<sup>1</sup>. As shown in Fig.1, seawater is pumped towards the first cell effect (or heater) of the MED. There, part of the water is evaporated and the rest of the seawater goes down to the following cells by gravity (a detailed description of the MED unit can be found in [11]). The required heat for the heater is provided by the solar field that supplies energy to the storage system (two 12 m<sup>3</sup> water storage tanks). A three-way regulation valve,  $V_M$ , is used to reach the nominal temperature at the inlet of the first effect, by mixing water from the primary tank with that returned from the heater. When the solar field temperature exceeds the one in the primary tank, the on-off valve position,  $V_t$ , is changed to connect these components. Otherwise, the solar field should be connected to the bottom part of the secondary water tank to avoid cooling down the primary water tank.

### 2.2 GREENHOUSE ENVIRONMENT

The research data used in this work have been obtained from greenhouses located in the Experimental Station of the Cajamar Foundation, El Ejido, in the province of Almería, Spain (2°43' W, 36°48' N, and at a 151-m elevation). The tomato crops are grown in a multi-span "Parral-type" greenhouse (Fig.2). The greenhouse has a surface area of 877 m<sup>2</sup> (37.8 x 23.2 m) with a polyethylene cover. The daytime air temperature and humidity are managed using the top and side windows which are controlled via a PI controller [17]. In addition, the biomass-based heating system allows one to control the night-time air temperature [20]. Setpoints for both systems are established at 24 °C, and 10 °C for the ventilation and heating, respectively. Throughout the experiments, the following inside climatic variables were continuously monitored: air temperature and relative humidity (Vaisala HMP45A), solar radiation (Delta-Ohm LP PYRA 03), and photosynthetic

<sup>1</sup>Although the system was designed to operate also with fossil energies [1], this work only deals with the solar operation mode.



Figure 2: Greenhouse facilities used for the experiences performed in this work. From left to right and from top to bottom: Greenhouse, Dropper, Solar and PAR radiation device at the outside, Irrigation system, Solar and PAR radiation device inside the greenhouse, and the tomato crop lines.

active radiation (PAR, Kipp&Zonen PAR-Lite). Outside the greenhouse a meteorological station was installed, in which air temperature, relative humidity, solar and photosynthetic active radiation, rain detection, wind direction, and velocity measurements were taken. The crop was grown in coconut coir bags with six plants and three droppers each. The irrigation is automated by a demand tray, which is formed by two crop bags. Drainage water is set at 20 % volume. All data are recorded every minute with a personal computer.

### 3 SOLAR DESALINATION PLANT MODEL

The model of the solar desalination plant is divided in three main components; the solar field, the storage system and the MED unit. Fig.3 shows a diagram with the connections between these models. A description of the variables involved is included in Table 1.

The solar field has been characterized using a concentrated parameter model based on energy balance, and the storage tanks have been characterized with models based on energy and mass balances. A description of these dynamic models can be found in [16]. With the aim of reducing the computational time of the whole model, a first-order model has been experimentally obtained to predict the distillate production (the distillate flow rate,  $q_d$ ) as a function of the inlet MED temperature,  $T_{iM}$ , and mass flow rate,  $\dot{m}_M$ :

$$q_d(s) = \frac{0.07}{120s + 1} e^{-100s} T_{iM}(s) + \frac{0.021}{60s + 1} e^{-40s} \dot{m}_M(s) \quad (1)$$

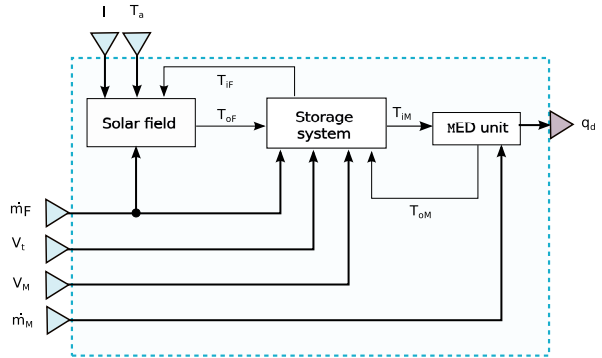


Figure 3: Connection between the submodels of the solar desalination plant.

Symbol	Description	Units	
$D$	Volume of water in the distillate tank	[m <sup>3</sup> ]	
$I$	Irradiance	[W/m <sup>2</sup> ]	
$\dot{m}$	Mass flow rate	[kg/s]	
$t_m$	Sampling time	[s]	
$T$	Temperature	[°C]	
$q$	Volumetric flow rate	[m <sup>3</sup> /h]	
Sub.	Description	Sub.	Description
0	Initial value	$a$	Ambient
$d$	Distillate	$F$	Solar field
$i$	Inlet	$M$	MED
$o$	Outlet	$p$	Primary tank
Superscript			Description
*			Setpoint

Table 1: Nomenclature

### 4 CONTROL SYSTEM

The idea behind the controller proposed in this section is to maintain a desired volume of distil-

late,  $D^*$ , by regulating the temperatures in the solar field and in the MED heater.

This controller (see Fig. 4) includes two loops:

- Loop 1: To reach the desired distillate demand, the solar field must deliver enough thermal energy. A NMPC is used to solve an optimization problem, calculate a reference for the outlet solar-field temperature and assure the required distillate production. This controller must be applied over the temperature instead of the water flow rate to include the following constraints:

$$1^\circ\text{C} \leq T_{oF}^* - T_{iF} \leq 20^\circ\text{C}, \quad (2)$$

$$T_p \leq T_{oF}^* \leq 95^\circ\text{C}. \quad (3)$$

The solar-field outlet-inlet temperature difference must be lower than  $20^\circ\text{C}$  to avoid stress in the absorber tubes, a minimum temperature difference must be guaranteed to avoid cooling down the water,  $T_{oF}$  must be under  $95^\circ\text{C}$  to avoid evaporation and it should be higher than  $T_p$  to not to cool down the stored water.

The outlet solar-field temperature,  $T_{oF}$ , may be controlled by varying the solar-field water mass flow rate,  $\dot{m}_F$ . Several algorithms have been tested in this plant, obtaining successful results [2, 13, 14, 15, 25, 21]. In this case, a feedback linearization control, FLC, is used [13].

- Loop 2: Since the distillate production depends mainly on the thermal energy delivered to the first effect, if nominal conditions are assumed in the MED mass flow rate,  $\dot{m}_M$ , a controller in  $T_{iM}$  is required to reach the desired demand. For this purpose, two consecutive PI's are included. The first one calculates a reference temperature for the MED inlet water,  $T_{iM}^*$ . This temperature is controlled with the second PI using the aperture of valve  $V_M$  as control variable.

Notice that there is a maximum temperature, to avoid scale formation in the heater,  $72^\circ\text{C}$ .

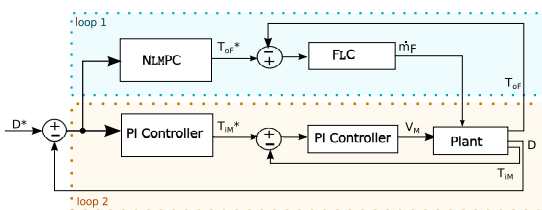


Figure 4: Control scheme

A minimum temperature is also defined to assure a minimum distillate production:  $55^\circ\text{C} \leq T_{iM}^* \leq 72^\circ\text{C}$ .

#### 4.1 NONLINEAR MPC

Model predictive control, MPC, is a typical control methodology that uses a model of the process to estimate the outputs at future time values  $\hat{y}(t+k|t)$  and calculate the optimal future inputs. In general, MPC algorithms consist of applying a control sequence that minimizes a cost function:

$$J = \sum_{j=N_1}^{N_2} \delta(j) [\hat{y}(t+k|t) - \omega(t+j)]^2 + \sum_{j=1}^{N_u} \lambda(j) [\Delta u(t+j-1)]^2, \quad (4)$$

where  $\omega$  is the reference signal,  $\Delta u$  is the control effort obtained from cost function minimization,  $N_1$  is the minimum prediction horizon,  $N_2$  is the maximum prediction horizon,  $N_u$  is the control horizon and  $\delta(j)$  and  $\lambda(j)$  are weighting sequences that penalize future tracking errors and control efforts, respectively, along the horizons.

Although most of the MPCs are applied to linear models, some techniques have been developed to obtain the future control actions using a nonlinear model of the process [3]. In this work, the NEPSAC approach has been chosen [5] because it uses directly the nonlinear prediction model without local linearization and it solves the optimization problem in a low computational time. The idea behind this technique is to use the nonlinear model to predict the base response and the step response.

For linear systems, the superposition principle is valid:

$$y(t+k|t) = y_{base}(t+k|t) + y_{opt}(t+k|t), \quad (5)$$

where  $y_{base}(t+k|t)$  is the effect of a base control sequence, and  $y_{opt}(t+k|t)$  is the effect of the optimized future control actions. This second component is the result of unit impulse ( $h_i$ ) and step responses ( $g_i$ ):

$$y_{opt}(t+k|t) = h_k \Delta u(t|t) + h_{k-1} \Delta u(t+1|t) + \dots + g_{k-N_u+1} \Delta u(t+N_u-1|t). \quad (6)$$

Using matrix notation, the vector of outputs is,

$$\mathbf{Y} = \bar{\mathbf{Y}} + \mathbf{G}\mathbf{U}, \quad (7)$$

where  $\bar{\mathbf{Y}}$ , is the vector of base response outputs from  $t+N_1$  through  $t+N_2$ ,  $\mathbf{U}$  is the vector of future controls up to  $t+N_u-1$  and  $\mathbf{G}$  is the  $(N_2-N_1+1) \times N_u$  matrix with impulse and step

response coefficients. Minimizing the cost function 4, a closed form solution can be obtained for the unconstrained case [6]:

$$\mathbf{U}^* = (\mathbf{G}^T \mathbf{G} + \lambda \mathbf{I})^{-1} \mathbf{G}^T (\mathbf{R} - \bar{\mathbf{Y}}). \quad (8)$$

The control input applied to the plant is,

$$u^*(t) = u_{base}(t|t) + \Delta u(t|t) = u_{base}(t|t) + \mathbf{U}^*(1). \quad (9)$$

In the case of nonlinear systems, since the superposition principle is no longer valid, the NEPSAC approach proposes to find iteratively a control input  $u_{base}(t+k|t)$  as close as possible to  $u^*(t+k|t)$  so that  $y_{opt}(t+k|t) \approx 0$  and the superposition principle is not involved. The procedure is the following one:

1. choose an initial  $u_{base}(t+k|t)$ , for example  $u_{base}(t+k|t) = u^*(t+k|t-1)$ ,
2. calculate  $\Delta u(t+k|t)$  as explained for the linear case,
3. if  $|\Delta u(t+k|t)| < \varepsilon$ , where  $\varepsilon$  is close enough to zero, then  $u^*(t+k|t) = u_{base}(t+k|t) + \Delta u(t+k|t)$  and the suboptimal control input is  $u^*(t+k|t)$ , otherwise make  $u_{base}(t+k|t) = u^*(t+k|t) + \Delta u(t+k|t)$  and go to step 2.

## 4.2 FEEDBACK LINEARIZATION CONTROL

The purpose of feedback linearization control is to transform a nonlinear system into a linear one using a nonlinear feedback that makes up for nonlinearities in system behavior [24]. This technique was applied to AQUASOL solar field to track a desired temperature reference using the water mass flow rate as the control signal [13]. Since experimental results showed successful results, this controller has been used in this work to follow the optimal references estimated by the NMPC.

## 4.3 PI CONTROLLERS

The second loop includes two PI controllers with anti-windup. The first one is used as a reference governor to choose the inlet MED temperature setpoint,  $T_{iM}^*$ . The parameters of this controller are:  $K_p=20^\circ\text{C}/\text{m}^3$ ,  $T_i=1200\text{ s}$  and  $T_t=15\text{ s}$ . The temperature setpoint obtained with this controller is reached using another PI controller that regulates the valve aperture,  $V_M$ . In this case, the parameters are:  $K_p=-2\%/^\circ\text{C}$ ,  $T_i=60\text{ s}$  and  $T_t=8\text{ s}$ .

## 5 SIMULATION RESULTS

In this section, a simulation is included to demonstrate the advantages of using the controllers to

calculate the solar-field and MED temperature setpoints. The results are compared with the case of using these setpoints fixed at  $72^\circ\text{C}$  (which is the maximum value considered as input in the MED unit).

With the aim of scaling the greenhouse water consumption to a real case, 6 greenhouses have been considered in the simulation. Therefore, the real consumption values obtained from the greenhouse have been multiplied for 6. Taking into account that typical daily consumption is around  $1.3\text{ m}^3$ , and assuming two days of storage capacity in case of cloudy days, the setpoint in the distillate volume has been established to  $D^* = 6 \cdot 1.3 \cdot 2 = 15.6\text{ m}^3$ .

The NMPC strategy was tested using the following tuning parameters:  $t_m = 300\text{ s}$ ,  $N_1 = 1\text{ s}$ ,  $N_2 = 600\text{ s}$ ,  $\delta = 0$  and  $\lambda(j) = 10^{-6}$ .

## 5.1 A TYPICAL OPERATION DAY

In this example the aim is to observe the controller response when the output is near the reference level. Real irradiance and water consumption are depicted in Fig.5, besides the volume of distillate obtained both with the controller and the open loop case.

At the beginning of the simulation, NMPC predicts that the optimal temperature reference is the minimum one (see Fig.6 (a)). Although the water mass flow rate is saturated at its maximum value (Fig.6 (c)) trying to follow the reference, the setpoint is not feasible with those conditions. Before reaching the distillate reference,  $T_{oF}^*$  starts to increase and  $\dot{m}_F$  decreases. Therefore, distillate production is slightly reduced because less thermal power is being delivered to the storage system. Nevertheless, at time 50506 s, the greenhouse irrigation system is turned on and the volume of stored distillate drastically decreases. For this reason, the optimal values obtained with NMPC are again near the minimum one. This procedure is repeated until the end of the simulation. For the open-loop case,  $\dot{m}_F$  is saturated for most part of the time (Fig.6 (d)) trying to follow the temperature setpoint (Fig.6 (b)).

The second control loop is shown in Fig.7. Whereas the MED setpoint is fixed for the case of the open-loop case (Fig.7 (b)), this value varies continually ((Fig.6 (a)) when the controller is applied and the volume of distillate is near the desired value. The aperture of the valve decreases when more water coming from the primary tank is needed to reach the desired temperature at the inlet of the MED unit.

Electricity consumption in the solar-field water

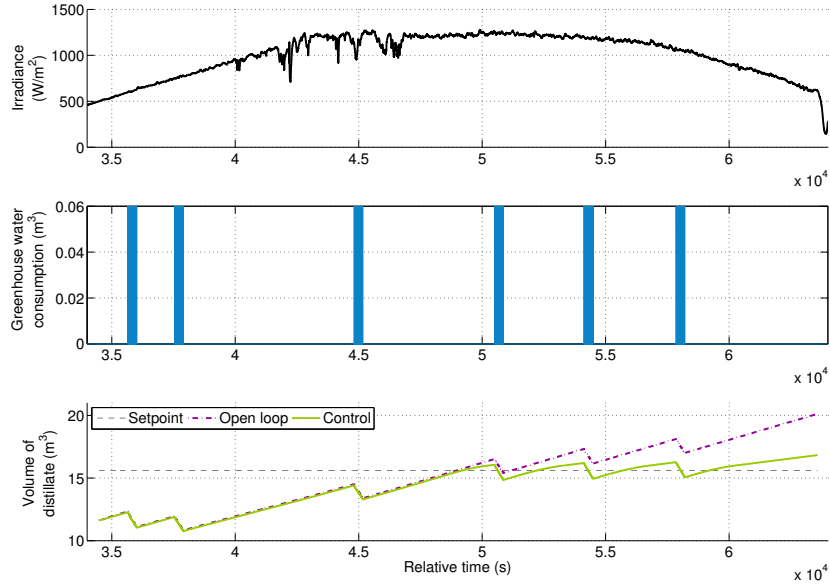


Figure 5: Irradiance and volume of distillate in a typical operation day.

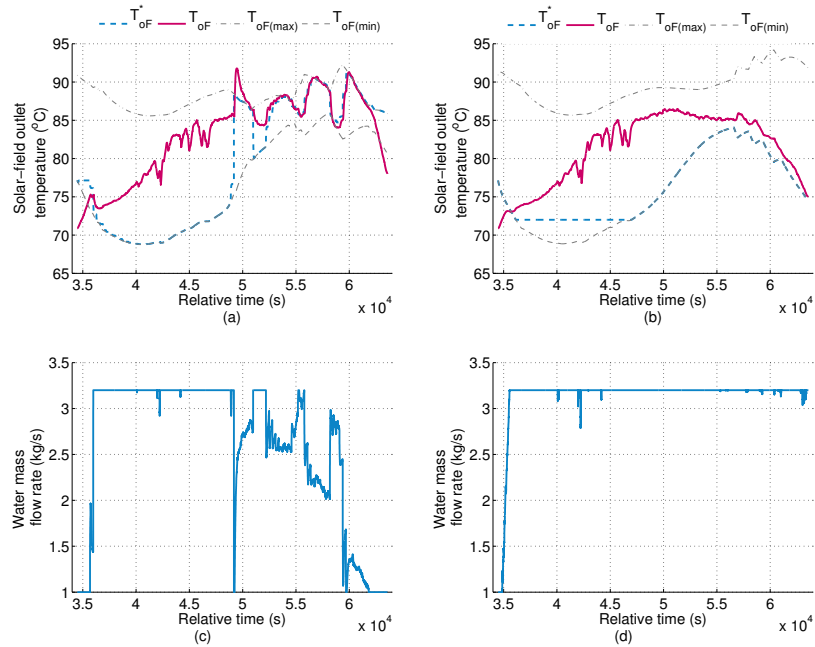


Figure 6: Solar-field temperature and water mass flow rate in a typical operation day. Control case (a) and (c). Open loop case (b) and (d).

pump is reduced as a consequence of using the controller to properly choose the setpoint values to maintain a desired volume in the distillate tank. Since less water flow rates are required, the pump is working at lower power levels which reduces the electricity costs.

## 6 CONCLUSIONS

For a specific greenhouse demanding water for irrigation purposes, to use distillate from a solar facility is a feasible process that must be controlled. The use of appropriate control techniques could not only assure the water demand, but also reduce electricity costs. The simulations shown in



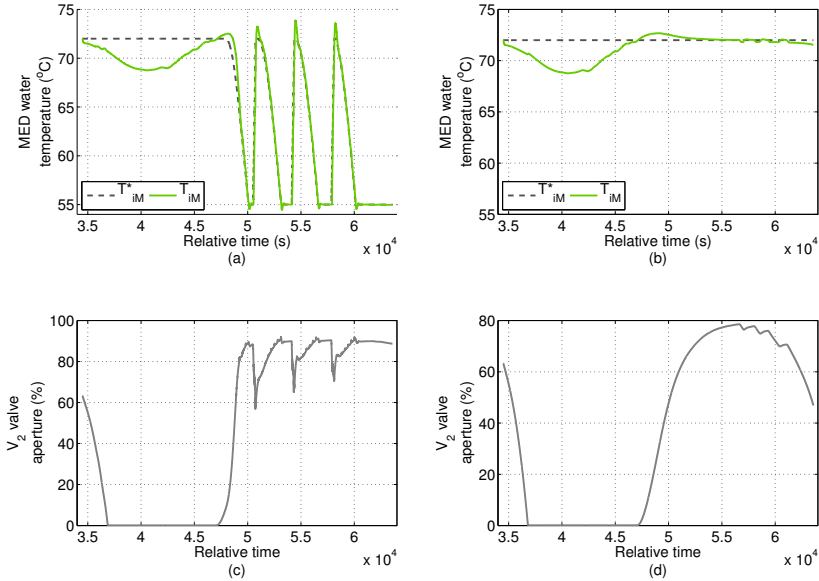


Figure 7: MED temperature and  $V_2$  valve aperture in a typical operation day. Control case (a) and (c). Open loop case (b) and (d).

this paper deal only with a typical operating day, but more simulations are required to evaluate the cost throughout one year taking into account water dependence of crops along the different seasons. Future works will also include a model of the greenhouse water consumption that will be used with two main purposes: i) use it as a load simulator for an experimental campaign in the solar desalination facility to evaluate the controller explained in this paper, ii) include it in the NMPC cost function to improve the estimations of the future control actions (the solar field temperature setpoints).

### Acknowledgments

This work has been funded by project DPI2010-21589-C05-02 financed by the Spanish Ministry of Economy and Competitiveness and ERDF funds and by the Controlcrop Project, P10-TEP-6174, project framework, supported by the Andalusian Ministry of Economy, Innovation and Science (Andalusia, Spain).

### References

- [1] D. Alarcon-Padilla, J. Blanco-Gálvez, L. García-Rodríguez, W. Gernjak, and S. Malato. First experimental results of a new hybrid solar/gas multi-effect distillation system: the AQUASOL project. *Desalination*, 220(1-3):619–625, 2008.
- [2] C. O. Ayala, L. Roca, J. L. Guzman, J. E.

Normey-Rico, M. Berenguel, and L. J. Yebra. Local model predictive controller in a solar desalination plant collector field. *Renewable Energy*, 36(11):3001–3012, 2011.

- [3] E. F. Camacho and C. Bordons. *Model predictive control*. Springer, 2013.
- [4] M. T. Chaibi. An overview of solar desalination for domestic and agriculture water needs in remote arid areas. *Desalination*, 127(2):119–133, 2000.
- [5] R. De Keyser. Model based predictive control. *UNESCO Encyclopaedia of Life Support Systems (EoLSS)*, 2003.
- [6] A. Dutta, R. De Keyser, and I. Nopens. Robust nonlinear extended prediction self-adaptive control (nepsac) of continuous bioreactors. In *20th Mediterranean Conference on Control & Automation (MED)*, pages 658–664. IEEE, 2012.
- [7] M. D. Fernández, A. M. González, J. Carreno, C. Pérez, and S. Bonachela. Analysis of on-farm irrigation performance in mediterranean greenhouses. *Agricultural Water Management*, 89(3):251 – 260, 2007.
- [8] M. F. A. Goosen, S. S. Sablani, C. Paton, J. Perret, A. Al-Nuaimi, I. Haffar, H. Al-Hinai, and W. H. Shayya. Solar energy desalination for arid coastal regions: development

- of a humidification–dehumidification seawater greenhouse. *Solar energy*, 75(5):413–419, 2003.
- [9] S. R. Hosseini, M. Amidpour, and S. E. Shakib. Cost optimization of a combined power and water desalination plant with energetic, environment and reliability consideration. *Desalination*, 285:123–130, 2012.
- [10] C. Li, Y. Goswami, and E. Stefanakos. Solar assisted sea water desalination: A review. *Renewable and Sustainable Energy Reviews*, 19:136–163, 2013.
- [11] P. Palenzuela, D. Alarcón, J. Blanco, E. Guillén, M. Ibarra, and G. Zaragoza. Modeling of the heat transfer of a solar multi-effect distillation plant at the Plataforma Solar de Almería. *Desalination and Water Treatment*, 31(1-3):257–268, 2011.
- [12] P. Paton, C. and Davies. The seawater greenhouse cooling, fresh water and fresh produce from seawater. In *The 2nd International Conference on Water Resources in Arid Environments, Riyadh*, 2006.
- [13] L. Roca, M. Berenguel, L. Yebra, and D. Alarcón-Padilla. Solar field control for desalination plants. *Solar Energy*, 82:772–786, 2008.
- [14] L. Roca, J. L. Guzman, J. E. Normey-Rico, M. Berenguel, and L. J. Yebra. Robust constrained predictive feedback linearization controller in a solar desalination plant collector field. *Control Engineering Practice*, 17(9):1076–1088, 2009.
- [15] L. Roca, J. L. Guzman, J. E. Normey-Rico, M. Berenguel, and L. J. Yebra. Filtered Smith predictor with feedback linearization and constraints handling applied to a solar collector field. *Solar Energy*, 85(5):1056–1067, 2011.
- [16] L. Roca, L. J. Yebra, M. Berenguel, and D. Alarcon-Padilla. Modeling of a Solar Seawater Desalination Plant for Automatic Operation Purposes. *Journal of Solar Energy Engineering*, 130(4):041009–1–041009–8, 2008.
- [17] F. Rodríguez, J.L. Guzmán, M. Berenguel, and M.R. Arahal. Adaptive hierarchical control of greenhouse crop production. *International Journal of Adaptive Control Signal Processing*, 22:180–187, 2008.
- [18] R. Salcedo, E. Antipova, D. Boer, L. Jiménez, and G. Guillén-Gosálbez. Multi-objective optimization of solar rankine cycles coupled with reverse osmosis desalination considering economic and life cycle environmental concerns. *Desalination*, 286:358–371, 2012.
- [19] F. Sánchez-Martos, A. Pulido, and J. M. Calaforra. Hydrogeochemical processes in an arid region of europe (almeria, {SE} spain). *Applied Geochemistry*, 14(6):735 – 745, 1999.
- [20] J. A. Sánchez-Molina, J. V. Reinoso, F. G. Ación, F. Rodríguez, and J. C. López. Development of a biomass-based system for nocturnal temperature and diurnal co2 concentration control in greenhouses. *Biomass and Bioenergy*, 67:60–71, 2014.
- [21] T. Santos, L. Roca, and J. L. Guzman. Practical mpc with robust dead-time compensation applied to a solar desalination plant. In *18th IFAC World Congress*, pages 4909–4914, 2011.
- [22] K. M. Sassi and I. M. Mujtaba. Optimal operation of ro system with daily variation of freshwater demand and seawater temperature. *Computers & Chemical Engineering*, 59:101–110, 2013.
- [23] S. E. Shakib, S. R. Hosseini, M. Amidpour, and C. Aghanajafi. Multi-objective optimization of a cogeneration plant for supplying given amount of power and fresh water. *Desalination*, 286:225–234, 2012.
- [24] J. Slotine and W. Li. *Applied nonlinear control*. Prentice Hall, 1991.
- [25] B. C. Torrico, L. Roca, J. E. Normey-Rico, J. L. Guzman, and L. J. Yebra. Robust Nonlinear Predictive Control Applied to a Solar Collector Field in a Solar Desalination Plant. *Control*, 18(6):1430–1439, 2010.
- [26] L. Wu, Y. Hu, and C. Gao. Optimum design of cogeneration for power and desalination to satisfy the demand of water and power. *Desalination*, 324:111–117, 2013.
- [27] M. Zamen, M. Amidpour, and M. R. Firoozjahi. A novel integrated system for fresh water production in greenhouse: Dynamic simulation. *Desalination*, 322:52–59, 2013.